JACS Au
AN OPEN ACCESS JOURNAL OF THE AMERICAN CHEMICAL SOCIETY

Editors' Choice
Open Access
This article is licensed under CC-BY-NC-ND 4.0
pubs.acs.org/jacsau
Article

Intracellular Delivery of Stabilized Peptide Blocking MTDH-SND1 Interaction for Breast Cancer Suppression

Hailing Chen, Meimiao Zhan, Yaping Zhang, Jianbo Liu, Rui Wang, Yuhao An, Zhanxia Gao, Leying Jiang, Yun Xing, Yibin Kang,* Zigang Li,* and Feng Yin*

Cite This: *JACS Au* 2024, 4, 139−149
Read Online

ACCESS | Metrics & More | Article Recommendations | Supporting Information

ABSTRACT: Triple-negative breast cancer is one of the most prevalent malignant cancers worldwide. Disrupting the MTDH-SND1 protein−protein interaction has recently been shown to be a promising strategy for breast cancer therapy. In this work, a novel potent stabilized peptide with a stronger binding affinity was obtained through rational structure-based optimization. Furthermore, a sulfonium-based peptide delivery system was established to improve the cell penetration and antitumor effects of stabilized peptides in metastatic breast cancer. Our study further broadens the in vivo applications of the stabilized peptides for blocking MTDH-SND1 interaction and provides promising opportunities for breast cancer therapy.

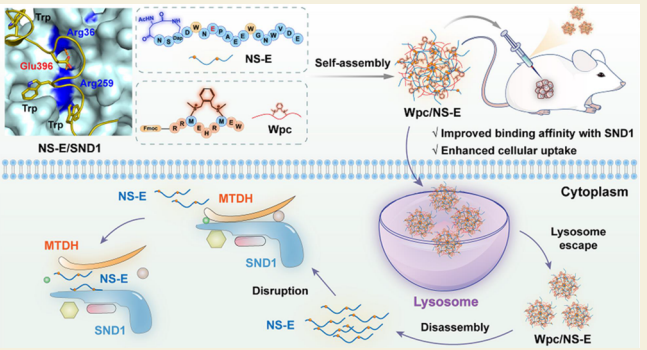

KEYWORDS: *MTDH-SND1 interaction, stabilized peptide, peptide delivery, in vivo, breast cancer therapy*

INTRODUCTION

Triple-negative breast cancer (TNBC) is the most prevalent malignant subtype of breast cancer which lacks effective targeted therapy.[1] Metadherin (MTDH) is upregulated in many types of malignant tumors.[2−4] *Staphylococcal* nuclease domain-containing protein 1 (SND1) is also highly expressed in different cancers, such as breast cancer, hepatocellular carcinoma, clear cell renal cell carcinoma (ccRCC), et al.[5−7] MTDH-SND1 protein−protein interaction plays a crucial role in breast cancer occurrence, development, drug resistance, prognosis, etc.[8−12] Small molecules targeting the MTDH-SND1 complex have shown promising therapeutic potential for treating TNBC.[9,10] In addition to small molecules, stabilized peptides harnessing larger interaction surfaces and stable secondary conformations could also disrupt MTDH-SND1 interaction effectively due to their stronger binding ability and high selectivity.[13] Recently, our group reported a 15-mer peptide MS2D derived from MTDH, which exhibited strong binding affinity to SND1.[13] Based on the MS2D sequence, a novel class of stabilized peptides was generated, and two candidate peptides were chosen for TNBC treatment. Although stabilized peptides demonstrated potential antitumor effects in breast cancer treatment, they still exhibited limited bioactivity and functioned with high doses. This limitation may be partly due to the nature of SND1 surfaces, which favored peptide ligands with more negative charges involved. As a result, the designed peptides faced challenges of relatively poor cell and tissue penetration. Hence, it is important to develop a safe delivery system to render bioactive peptides more cell-permeable, which could further broaden their in vivo and clinical applications.

Current strategies for peptide delivery rely on nanocarriers, such as polymeric materials, inorganic nanoparticles or lipid-based nanocarriers, etc.[14−20] Although these methods exhibit satisfying effects in peptide delivery, the synthesis of some materials is complicated and drug assembly is often performed in organic solvents, resulting in the decrease of peptide bioactivity.[21,22] As alternative approaches, peptide carriers, such as cell-penetrating peptides (CPPs), are versatile carriers to deliver biomolecules such as peptides, proteins, and nucleic acids to targeted sites through covalent or noncovalent attachments in vitro and in vivo.[23−25] Nevertheless, CPPs used for covalent conjugation may hinder the targeting binding sites or disrupt the conformation of peptides. Moreover, attaching to CPPs may affect peptide subcellular localization and cytotoxicity.[26,27] As noncovalent nanocarriers, CPPs also present some limitations including low cytosolic delivery efficiency, endosomal entrapment, poor stability, etc.,[28,29] which further limits their applications.

In 2019, our group utilized the Met bis-alkylation strategy to develop a 9-mer cyclized peptide (Wpc) as a nanocarrier for

Received: September 27, 2023
Revised: November 10, 2023
Accepted: November 13, 2023
Published: December 8, 2023

© 2023 The Authors. Published by American Chemical Society

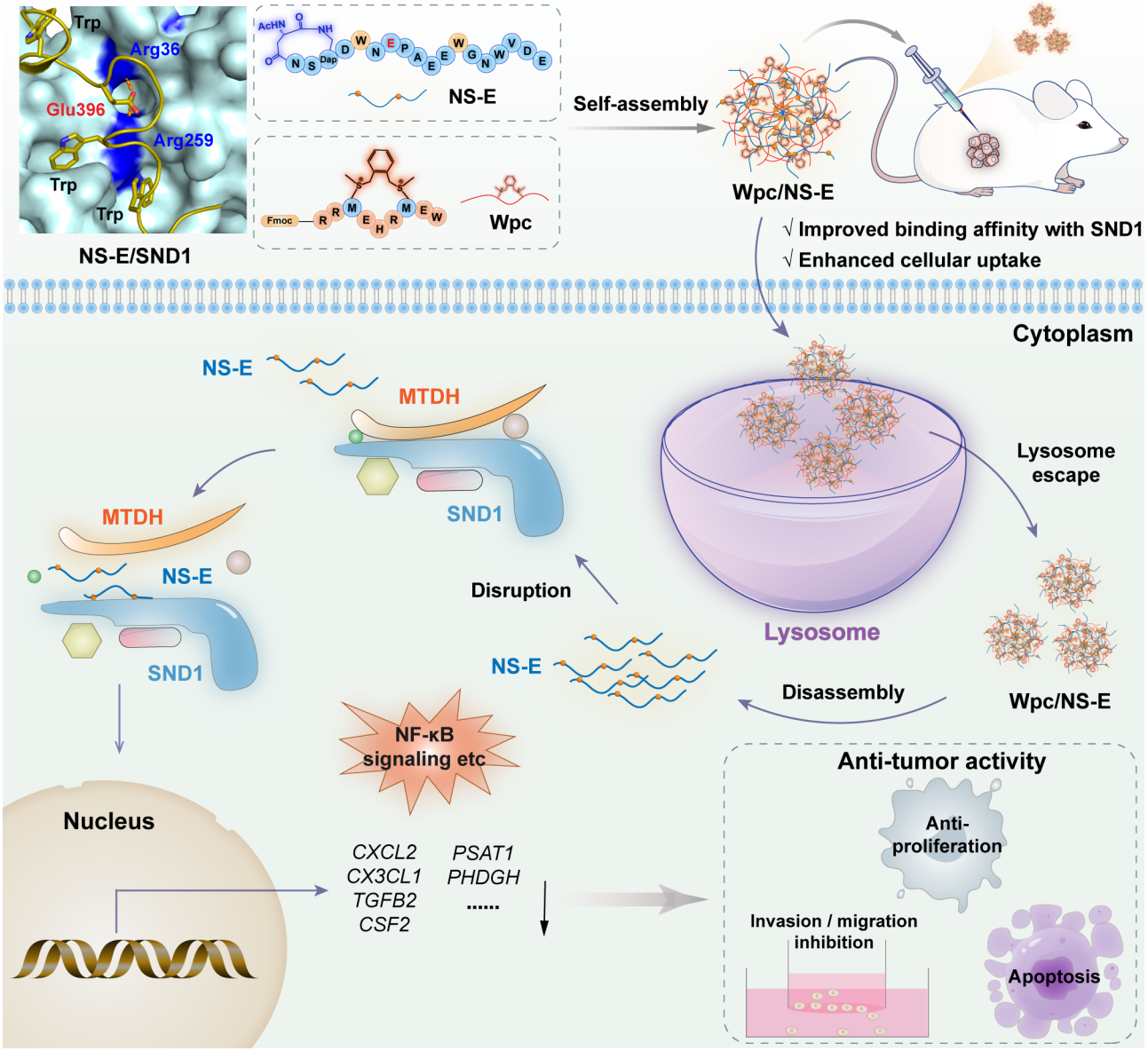

Figure 1. Schematic illustration of intracellular delivery of stabilized peptide targeting MTDH-SND1 complex for breast cancer therapeutics. Through introducing mutation and TD strategy, a stabilized peptide (NS-E) was obtained with better binding affinity (~23 nM). Glu396 of NS-E could enter into a positive charge center and strengthen the electrostatic interactions with SND1. To further improve the cell penetration of NS-E, the sulfonium-modified constrained peptide (Wpc) was utilized in assembling peptide nanoparticles (Wpc/NS-E) with NS-E to deliver NS-E into tumor cells. Wpc/NS-E nanoparticles could achieve lysosomal escape and release NS-E into the cytosol to disrupt MTDH-SND1 interaction, resulting in excellent antitumor activities in triple-negative breast cancer therapy.

nucleic acid drug delivery.[30−32] Wpc is a reversible sulfonium-based peptide carrier and could achieve highly efficient and controllable drug release in tumor microenvironment.[31,32] The sulfonium positive center of Wpc increases its hydrophobicity and positive charge, making it more effective in assisting the assembly of negatively charged biomolecules, including peptides (Figure 1). To maximize the therapeutic efficacy in cancer therapy, we herein reported a constrained peptide delivery system based on the Wpc nanocarrier to improve the cell penetration efficiency of stabilized peptides. Furthermore, the in vivo antitumor activity of stabilized peptides was also investigated (Figure 1). This peptide delivery system might provide more references to develop effective and selective therapeutic agents to treat TNBC.

RESULTS AND DISCUSSION

Peptide Design and Optimization

In the previous work, a series of peptide sequences were designed and optimized according to the MTDH-SND1 structure (PDB code: 4QMG).[12,13] Among these peptides, a 15-mer peptide named MS2D (D_{393}WNAPAEEWGNWVDE$_{407}$) was obtained with the strongest SND1 binding affinity (~60 nM).[13] Based on the docking structure of MS2D/SND1 (Figure S1), Ala396 of MS2D was located in a positive center contoured by Arg36 and Arg259 of SND1, so mutating Ala396 to negatively charged residues may improve the peptide binding affinity with SND1 through strengthening the electrostatic interactions. Moreover, extending the length of the side chain of Ala will increase the

https://doi.org/10.1021/jacsau.3c00573
JACS Au 2024, 4, 139−149

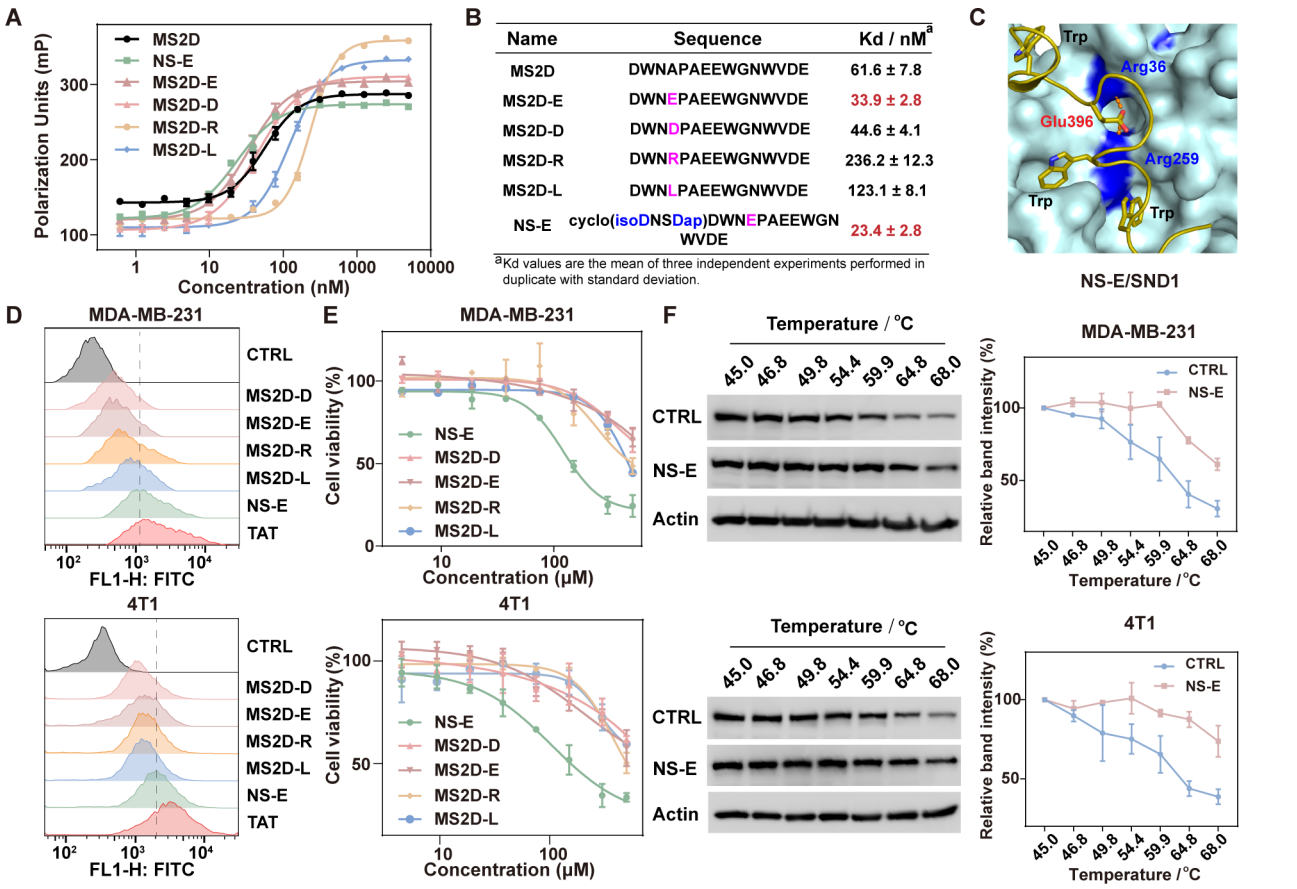

Figure 2. Peptide design and optimization. (A) Binding abilities of optimized peptides evaluated by the fluorescence polarization assay. (B) Sequences and K_d values of optimized peptides based on MS2D. (C) NS-E/SND1 docking structure. NS-E (dark yellow) and SND1 (pale cyan surface) were shown in the figure. (D) Cellular uptake efficiency of optimized peptides (20 μM) incubated with MDA-MB-231 and 4T1 cells for 12 h. (E) Cell viability of MDA-MB-231 and 4T1 cells upon treatments with optimized peptides at different concentrations for 72 h. (F) Cellular thermal shift assay of NS-E (120 μM) in MDA-MB-231 and 4T1 cells for 24 h.

opportunity to interact with Arg36 and Arg259 of SND1. In order to verify our hypothesis, starting from MS2D, Ala396 was mutated to acidic amino acids such as Glu (MS2D-E) or Asp (MS2D-D) in order to enhance the electrostatic interaction with the basic surface of SND1. Furthermore, MS2D-R and MS2D-L were synthesized for comparison to further validate the necessity of negatively charged residues applied in SND1 binding. Among these peptides, MS2D with lengthened side chain mutation (MS2D-E) exhibited stronger binding affinity, with a K_d value of ~34 nM (Figure 2A,B). Conversely, MS2D-L and MS2D-R showed almost twofold and fourfold decreases in binding ability compared with MS2D, respectively (Figure 2A,B), which was consistent with the assumption above.

To stabilize the conformation of MS2D-E, a lactam cyclization cap was introduced on the N-terminus of MS2D-E (NS-E-cyc, also named as NS-E), which was previously reported as an efficient stabilization methodology for the peptide structure (TD strategy).[33] The cyclized peptide NS-E with a K_d value of 23.4 ± 2.8 nM, improved the binding ability of linear peptide MS2D-E and exhibited a nearly threefold stronger binding affinity compared with MS2D (Figure 2B). According to the docking analysis, stabilized peptide NS-E could effectively bind with SND1, with key tryptophans (Trp394 and Trp401) entering into two dominant hydrophobic pockets. Additionally, Glu396 could reach into the basic groove and form electrostatic interaction with Arg36 and Arg259 of SND1, underlying the enhanced binding ability of NS-E (Figure 2C).

We next explored the cell permeability of NS-E in two types of TNBC cells (human MDA-MB-231 cells and mouse 4T1 cells) utilizing TAT as a positive control. It was found that NS-E displayed enhanced cell penetration efficiency compared with that of mutated linear peptides under the same concentration. However, NS-E still showed poor cellular uptake compared with TAT, especially in 4T1 cells (Figures 2D and S2). To investigate the response of cancer cells treated with optimized peptides, the cell counting kit-8 (cck8) assay was performed to examine the viability of breast cancer cells and normal human cells (MCF10A) after being incubated with peptides for 72 h. The optimized peptides, especially the stabilized peptide NS-E, exhibited potential antiproliferative activity in breast cancer cells, with an IC_{50} value of 121 μM in MDA-MB-231 and 103 μM in 4T1 cells (Figure 2E). Nevertheless, NS-E showed negligible antiproliferation effects on MCF10A cells even at the concentration of 300 μM, suggesting its selectivity and low toxicity (Figure S3). Cellular thermal shift assay demonstrated that stabilized peptide NS-E could effectively bind with SND1 in MDA-MB-231 and 4T1 cells, which could make it a promising peptide candidate for further study (Figure 2F).

https://doi.org/10.1021/jacsau.3c00573
JACS Au 2024, 4, 139−149

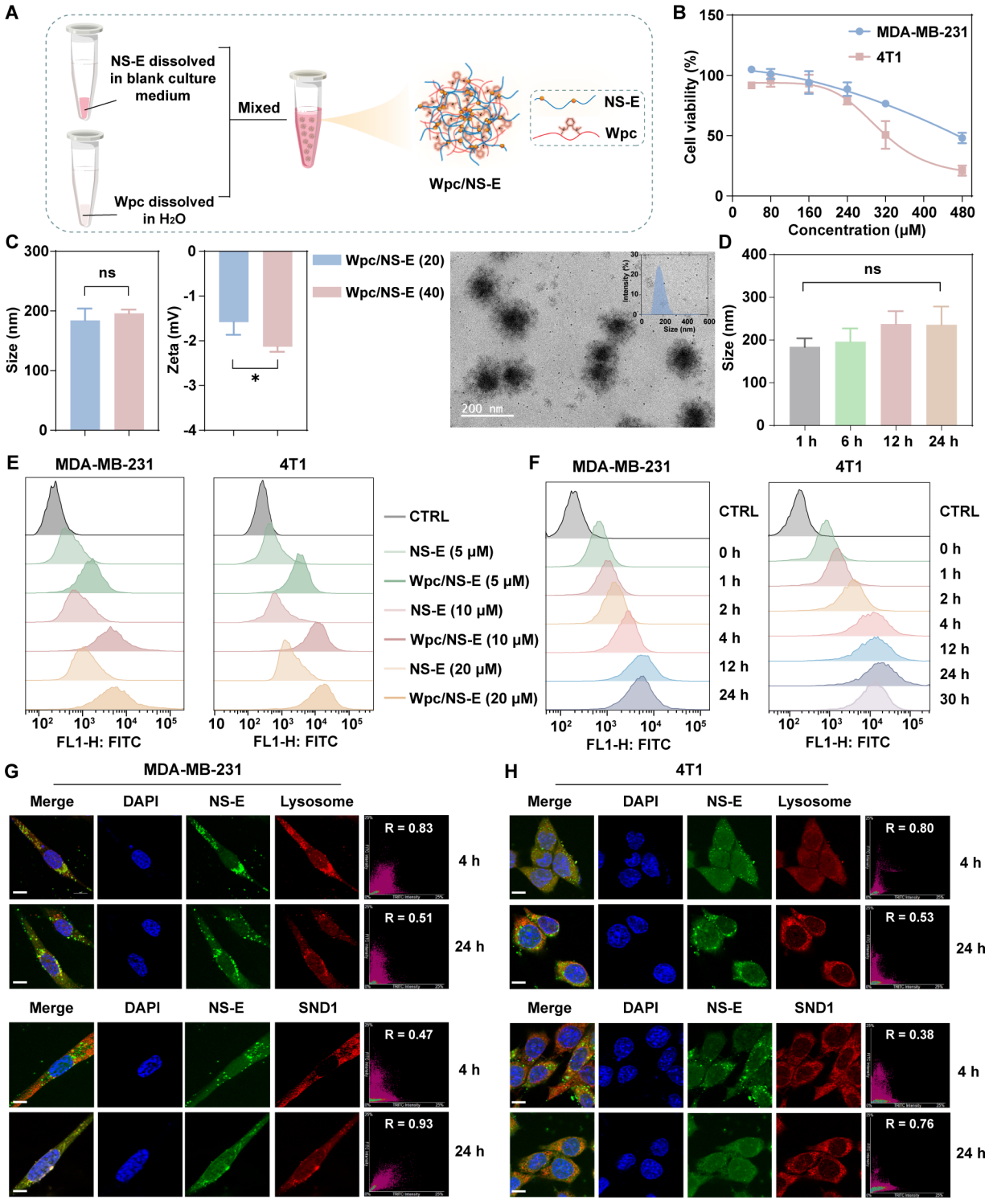

Figure 3. Design, characterization, and cellular permeability of Wpc/NS-E nanoparticles. (A) Scheme illustrated the assembly process of stabilized peptide NS-E and Wpc carrier. (B) Cell viability of MDA-MB-231 and 4T1 cells when treated with the Wpc nanocarrier at different concentrations. (C) Particle size, zeta potential, and TEM characterization of Wpc/NS-E with different ratios. Scale bar = 200 nm. (D) Particle size changes of Wpc/NS-E in 24 h. (E) Cellular uptake efficiency of NS-E and Wpc/NS-E incubated with MDA-MB-231 and 4T1 cells for 12 h. (F) Flow cytometry analysis of intracellular uptake of NS-E (20 μM) after mixing with Wpc at varying incubation time points. (G, H) CLSM analysis of the cellular distribution of NS-E in 4 and 24 h. Scale bar = 10 μm.

Design, Characterization and Cellular Permeability of Wpc/NS-E Nanoparticles

To improve the cellular uptake efficiency of stabilized peptide NS-E, nanocarriers with low cytotoxicity were considered to assemble with NS-E to avoid decreasing the binding ability via covalently fusing with CPP sequences (TAT, etc.).

Due to the presence of the abundant negatively charged amino acids and three tryptophans in the NS-E sequence, we utilized a 9-mer constrained peptide (Wpc) previously

https://doi.org/10.1021/jacsau.3c00573
JACS Au 2024, 4, 139−149

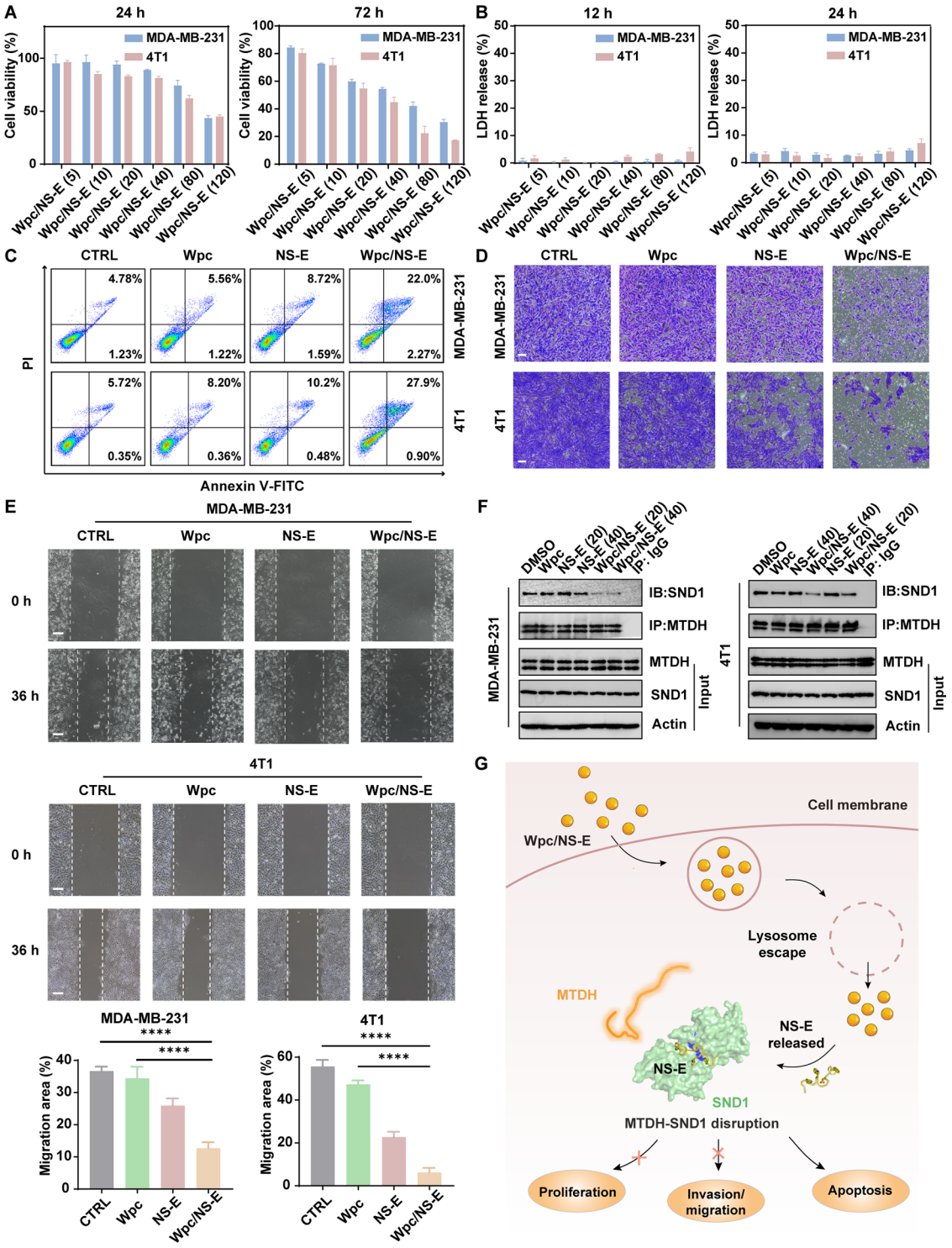

Figure 4. Antitumor effects of Wpc/NS-E in triple-negative breast cancer cells. (A) Cell viability of MDA-MB-231 and 4T1 cells when treated with Wpc/NS-E at 5, 10, 20, 40, 80, and 120 μM for 24 and 72 h. (B) LDH release assay. Wpc/NS-E at various concentrations were added to breast cancer cells for 12 and 24 h. (C) Flow cytometry analysis of MDA-MB-231 and 4T1 cells labeled with Annexin V-FITC and PI in different groups. (D) Images of transwell invasion assay on MDA-MB-231 and 4T1 cells in 36 h. Scale bar = 100 μm. Images were analyzed by ImageJ. (E) Images of wound-healing assays. Scale bar = 100 μm. Images were analyzed by ImageJ. One-way ANOVA multiple comparisons were used for statistical analysis (****p < 0.0001). (F) Co-IP assay in MDA-MB-231 and 4T1 cells. DMSO, Wpc, NS-E, and Wpc/NS-E at various concentrations were added to MDA-MB-231 and 4T1 cells for 24 h, respectively. (G) Schema illustration showed that Wpc delivered NS-E into cells and disrupted the MTDH-SND1 interaction, which induced apoptosis, further inhibited invasion and migration, and exerted antiproliferation effects in breast cancer cells.

developed by our group as a carrier to deliver peptide NS-E into cells (Figure 3A).

Prior to establishing a suitable concentration of the peptide delivery system, breast cancer cells were incubated with Wpc nanocarriers for 72 h to evaluate their cytotoxicity. The cell

https://doi.org/10.1021/jacsau.3c00573
JACS Au 2024, 4, 139−149

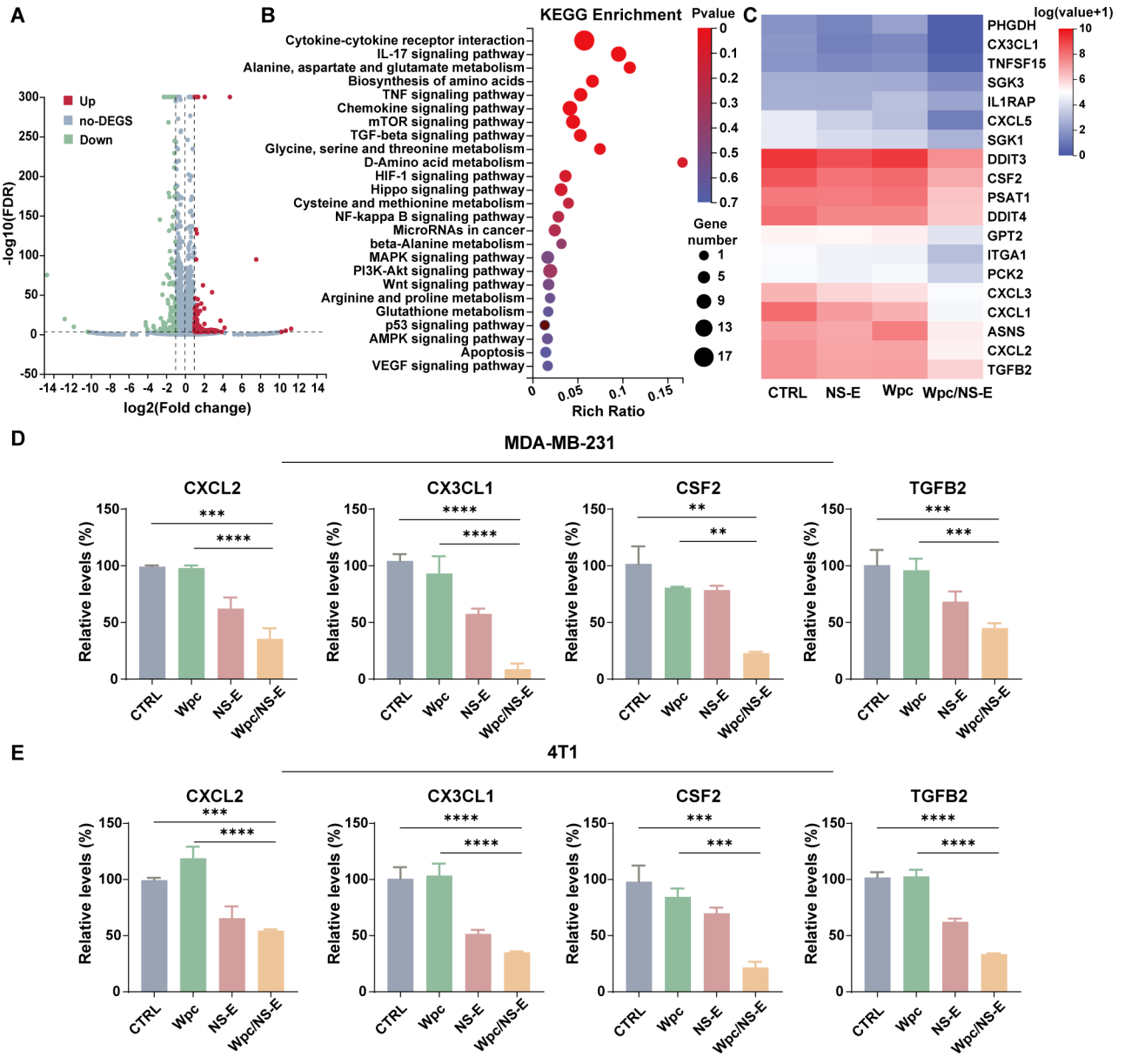

Figure 5. Transcriptome analysis. (A) Volcano plot of the differentially expressed genes (DEGs) in the Wpc and Wpc/NS-E groups. (B) KEGG analysis of different signaling pathways in Wpc/NS-E versus Wpc group. (C) Heat map of the DEGs identified by RNA-Seq in MDA-MB-231 cells after diverse treatments. (D, E) Intracellular mRNA level of chemokine-related genes (CXCL2, CX3CL1, CSF2, and TGFB2) in MDA-MB-231 and 4T1 cells after treatments with DMSO, Wpc, NS-E, and Wpc/NS-E. Error bars indicated mean ± SD ($n = 3$). One-way ANOVA multiple comparisons were used for statistical analysis (**$p < 0.01$, ***$p < 0.001$, ****$p < 0.0001$).

viability was over 85% at the concentration of 240 μM in MDA-MB-231 and 4T1 cells (Figure 3B). To avoid the cytotoxicity caused by an excessive Wpc carrier, NS-E peptide was diluted in a blank culture medium and mixed with a Wpc carrier (240 μM). After one-step mixing at RT for 1 h, the Wpc/NS-E nanoparticles at different ratios were formed uniformly with a diameter of nearly 200 nm according to the dynamic light scattering (DLS) analysis and TEM image (Figure 3C). The average zeta potential of the Wpc/NS-E nanoparticles was about −2 mV (Figure 3C). Moreover, the particle size of Wpc/NS-E remained stable in 24 h, suggesting its desirable stability at RT (Figures 3D and S4). To evaluate the intracellular delivery efficiency of Wpc/NS-E nanoparticles, MDA-MB-231 and 4T1 cells were treated with Wpc/NS-E at different concentrations for 12 h, respectively. Wpc/NS-E demonstrated significantly improved cellular uptake efficiency compared with NS-E alone, suggesting the potential of Wpc for intracellular delivery of peptides (Figures 3E and S5). According to flow cytometry analysis, Wpc/NS-E could reach the maximal cellular uptake within 12 h in MDA-MB-231 cells and 24 h in 4T1 cells (Figures 3F and S6).

To investigate the intracellular distribution of NS-E peptide in breast cancer cells, confocal laser scanning microscopy (CLSM) was used to observe the treated cells at different time points (4 and 24 h). It was found that the Wpc carrier could effectively deliver the NS-E into the cells and colocalize with lysosomes in 4 h (Figure 3G,H). Moreover, it was observed that with prolonged time, a good colocalization between NS-E and SND1 was observed, suggesting that Wpc/NS-E could achieve lysosome escape and release NS-E into the cytosol to bind with SND1 in

https://doi.org/10.1021/jacsau.3c00573
JACS Au 2024, 4, 139−149

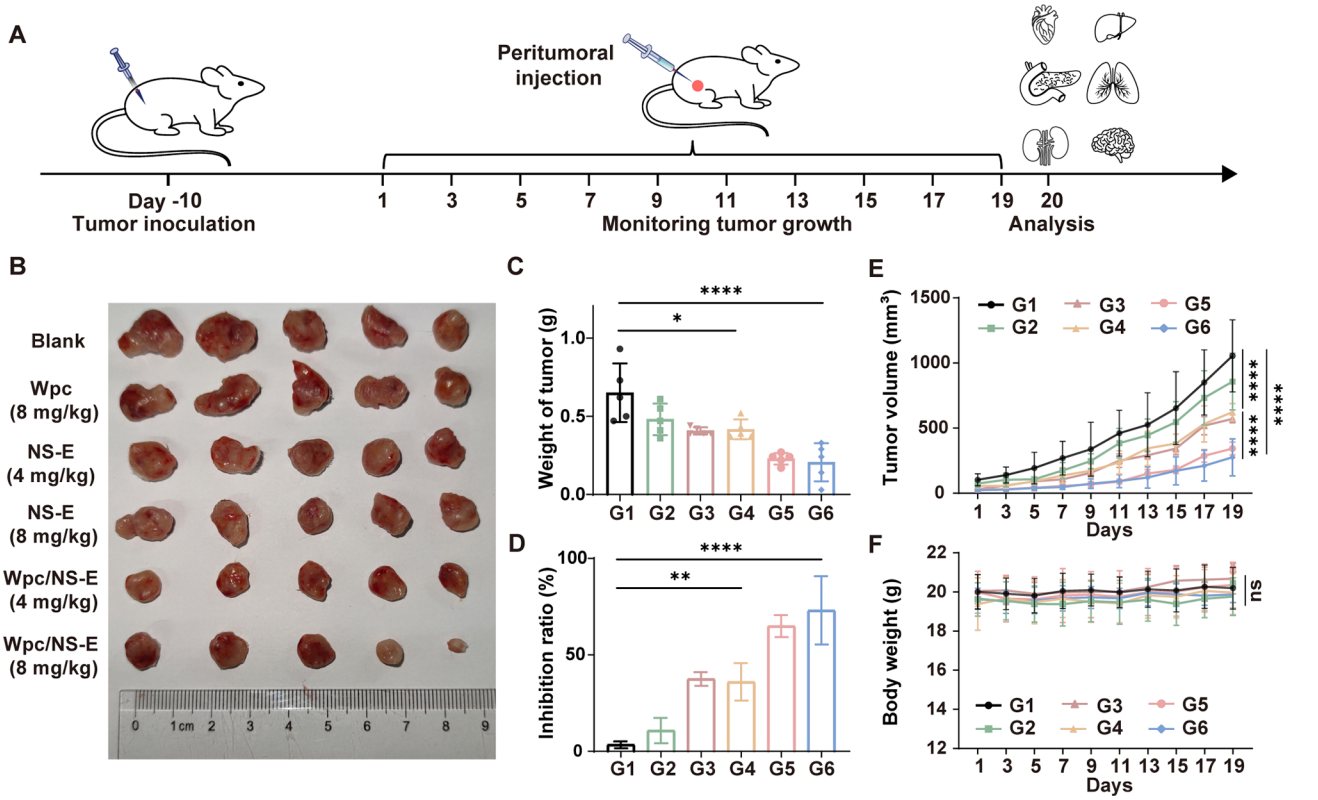

Figure 6. In vivo antitumor efficacy and biosafety study in 4T1-luc bearing mice. (A) Schematic diagram of primary tumor treatment in 4T1-luc bearing mice. (B) Images of tumor tissues treated with blank culture medium, Wpc (8 mg/kg), NS-E (4 mg/kg), NS-E (8 mg/kg), Wpc/NS-E (4 mg/kg), and Wpc/NS-E (8 mg/kg) by peritumoral injection, respectively. (C) Tumor weights of mice in different treatment groups. (D) Inhibition rates of tumor growth in different treatment groups. (E) Tumor volume changes in different groups. (F) Body weights of the mice after 19-day treatment in different groups. G1: Blank control, G2: Wpc (8 mg/kg), G3: NS-E (4 mg/kg), G4: NS-E (8 mg/kg), G5:Wpc/NS-E (4 mg/kg), and G6: Wpc/NS-E (8 mg/kg). Error bars indicated mean ± SD ($n = 3$). One-way ANOVA multiple comparisons were used for statistical analysis (ns: not significant, *$p < 0.05$, **$p < 0.01$, ***$p < 0.001$, ****$p < 0.0001$).

24 h (Figure 3G,H). 3D-z stacking scanning imaging also suggested that NS-E could colocalize with SND1 after Wpc/NS-E treatment for 24 h (Figure S7).

Wpc/NS-E Nanoparticle Induced Apoptosis and Inhibited Invasion and Migration of Breast Cancer Cells

Encouraged by the improved cellular uptake of NS-E, we started to evaluate the antitumor activity of Wpc/NS-E in breast cancer cells (MDA-MB-231 and 4T1) and normal human mammary epithelial cells (MCF10A). As shown in Figure 4A, Wpc/NS-E treatment could induce antitumor activity in a time-dependent manner. Upon incubation at various concentrations, Wpc/NS-E resulted in proliferation inhibition with the dose increasing in MDA-MB-231 and 4T1 cells in 72 h, respectively (Figure 4A). LDH release assay revealed that the in vitro antitumor effect of Wpc/NS-E was not owing to the nonspecific toxicity caused by cell membrane disruption (Figure 4B). Notably, no obvious cytotoxicity was observed in Wpc/NS-E-treated MCF10A cells (Figure S8), suggesting the selectivity and biosafety of Wpc/NS-E in breast cancer therapy.

Consistent with its tumor-suppression effects, the Wpc/NS-E treatment induced significant apoptosis in breast cancer cells (Figure 4C). Subsequently, to investigate whether Wpc/NS-E had the potential to inhibit tumor metastasis, a transwell invasion assay was conducted. The results demonstrated that the Wpc/NS-E treatment significantly repressed the invasion tendency in MDA-MB-231 and 4T1 cells (Figures 4D and S9). Supplementarily, the wound-healing analysis also demonstrated that Wpc/NS-E effectively enhanced tumor migration suppression, while the Wpc carrier showed little effect compared with the control group (Figure 4E). This finding further implicated that the peptide NS-E could effectively inhibit the migration and invasion of breast cancer cells.

To further explore the molecular mechanism of Wpc/NS-E-induced inhibition on breast cancer cell proliferation, the coimmunoprecipitation (Co-IP) assay was performed in breast cancer cells to examine the level of SND1 binding to MTDH. As shown in Figure 4F, compared to the NS-E group, the Wpc/NS-E-treated group showed stronger inhibitory effects on MTDH-SND1 formation without affecting the MTDH expression, indicating that the peptide NS-E could be delivered into breast cancer cells effectively and block MTDH-SND1 interaction through targeting SND1.

Collectively, these results suggested that Wpc could efficiently enhance the cell permeability of peptide NS-E and augment cytotoxicity against breast cancer cells by blocking the MTDH-SND1 interaction (Figure 4G). The same trend was also found in inhibiting the migration and invasion of TNBC cells (Figure 4G). These findings indicated that the Wpc-peptide assembled system could be a promising strategy to deliver stabilized peptide NS-E into tumor cells for improving treatment efficacy and lowering the therapeutic dose.

Transcriptome Analysis

To further elucidate the cellular functions of breast cancer cells upon treatment with Wpc/NS-E, transcriptome profiling was

https://doi.org/10.1021/jacsau.3c00573
JACS Au 2024, 4, 139−149

analyzed by RNA sequencing (RNA-Seq) in MDA-MB-231 cells. According to the volcano plot, RNA-Seq analysis identified 251 differentially expressed genes (DEGs) in the group of Wpc versus Wpc/NS-E, among which 123 genes were upregulated and 128 genes were downregulated ($p < 0.05$, $\log_2$ |fold change| > 1) (Figure 5A). In addition, 117 DEGs were detected in the groups Wpc/NS-E versus CTRL, Wpc/NS-E versus Wpc, Wpc/NS-E versus NS-E, and Wpc versus CTRL (Figure S10). Kyoto Encyclopedia of Genes and Genomes (KEGG) analysis revealed that DEGs were mainly enriched in the pathways of cell growth and death, signal transduction, cancer overview, amino acid metabolism, and immune system (Figure S11). MTDH could facilitate tumor progression and play an essential role in multiple signaling networks (including PI3K/Akt, NF-κB, Wnt signaling, etc.).[34−36] RNA-Seq analysis also demonstrated that several canonical oncogenic cellular pathways, including TNF, TGF-beta, NF-κB, PI3K-Akt signaling pathways, etc., were significantly enriched after treatment with Wpc/NS-E (Figure 5B). In addition, chemokine genes, such as CXCL1, CXCL2, CXCL3, CXCL5, CX3CL1, CSF2, and IL-6, were dramatically downregulated (Figure 5C). Most of them were NF-κB downstream target genes, which were reported to be responsible for the proliferation, survival, and invasion of breast cancer.[37−40] This finding indicated that Wpc/NS-E might downregulate oncogene-related chemokine expression via inhibition of NF-κB downstream signaling pathways. Moreover, TGFB2 was also observed in the DEGs, which could mediate TGF-beta, NF-κB, and other immune signaling pathways.[41−44] Next, we chose additional downstream candidate genes, including CXCL2, CX3CL1, CSF2, and TGFB2 for further validation. RT-qPCR results showed that the expressions of these genes were reduced significantly in MDA-MB-231 and 4T1 cells, consistent with the heatmap analysis (Figure 5D,E). Furthermore, other genes related to the biosynthesis and metabolism of amino acids were also investigated, such as PHGDH and PSAT1. Notably, as shown in Figure S12, Wpc/NS-E treatment enhanced the inhibition rates of PHGDH and PSAT1 (<40%) compared with NS-E alone. Above all, the MTDH-SND1 complex played a multifunctional role in tumor progression and its blockage might regulate oncogene-related signal transduction pathways involved in tumor growth and metastasis.

In summary, MTDH-derived stabilized peptide NS-E could inhibit tumor growth and invasion by regulating the MTDH-mediated signaling pathways associated with tumorigenesis, such as NF-κB signaling, PI3K/Akt, etc. However, how NS-E binds to SND1 and inactivates related signaling pathways (NF-κB, etc.) remains unclear at this point. More proof was necessary to gain a better understanding of NS-E mediated NF-κB/PI3K/Akt signaling inhibition through disrupting MTDH-SND1 interaction.

In Vivo Antitumor Efficacy and Biosafety Study

To investigate the antitumor effects of Wpc/NS-E in vivo, 4T1-luc mouse mammary tumor cells were subcutaneously injected into BALB/c mice to mimic TNBC.[45] When the tumor volume reached about 100 mm^3, BALB/c mice above were randomly divided into six groups ($n = 5$) and were peritumorally injected with blank culture medium, Wpc carrier (8 mg/kg), peptide NS-E (4 and 8 mg/kg), or Wpc/NS-E (4 and 8 mg/kg), respectively. Treatment was administered every other day for 19 days. Tumor size and body weight were measured before each treatment (Figure 6A). As illustrated in Figures 6B and S13, mice treated with only peptide NS-E exhibited potential tumor inhibition, even at a low dose of 4 mg/kg. Increasing the dose of NS-E (8 mg/kg) did not cause obvious toxicity, which further revealed that peptide NS-E could be well tolerated in mice. Furthermore, mice treated with Wpc/NS-E (at both 4 and 8 mg/kg) showed significantly enhanced antitumor effects with tumor inhibition rates of approximately 65 and 70%, respectively (Figure 6C,D). In contrast, Wpc treatment failed to suppress the tumor growth compared to Wpc/NS-E, suggesting that the in vivo antitumor efficacy caused by Wpc/NS-E was due to NS-E treatment instead of Wpc carriers (Figure 6E). In addition, no significant weight changes were observed in mice of each group after 19 days of administration (Figure 6F), confirming the low toxicity of NS-E and Wpc/NS-E.

To further verify the biocompatibility of Wpc/NS-E in 4T1-luc tumor-bearing mice, all the mice were euthanized to collect their hearts, livers, spleens, lungs, kidneys, and brains for analysis after the 19-day treatment. Then, hematoxylin and eosin (H&E) staining was utilized to detect the organ damages. After 19 days of treatment, the main organs of mice in each group showed negligible damage (Figure S14), fully demonstrating the in vivo safety of the peptide NS-E and Wpc/NS-E nanoparticles.

Overall, the data above indicated that Wpc could increase the tumor penetration efficiency of NS-E and inhibit tumor proliferation in vivo with good biocompatibility.

CONCLUSIONS

Blocking the MTDH-SND1 protein−protein interaction has recently been shown to be a promising strategy for TNBC therapy.[9,10,13,46] In this study, TD strategy was introduced to design a chemically modified stabilized peptide (NS-E) that can disrupt MTDH-SND1 interaction in breast cancer cells.[33] NS-E exhibited a fourfold enhancement of binding affinity compared with peptide inhibitors (MS2D-cyc4 and MS2D-cyc6) developed in the previous study.[13] However, NS-E showed poor cell penetration efficiency and exerted antitumor effects at a relatively high concentration, with an IC_{50} value of over 100 μM in MDA-MB-231 and 4T1 cells. Therefore, we established a stabilized peptide delivery system utilizing a reversible sulfonium-based peptide carrier (Wpc) to enhance the cell permeability of NS-E.

Further biological studies demonstrated that the Wpc nanocarrier could significantly enhance the cellular uptake efficiency of stabilized peptide NS-E and reduce its dosage (20 μM) in breast cancer therapy. Peptide NS-E could be delivered into tumor cells and effectively block the MTDH-SND1 interaction through targeting SND1. As a result, the Wpc/NS-E complex induced apoptosis and dramatically suppressed the proliferation, migration, and invasion of TNBC cells. Moreover, Wpc/NS-E also exhibited good therapeutic effects in the 4T1 TNBC mice model, further suggesting its excellent antitumor activity in vivo.

It was reported that MTDH was involved in the canonical oncogene-related pathways, including Wnt/β-catenin, NF-κB, PI3K/AKT, etc.[35,36,47,48] In addition, SND1-mediated ERK signaling and EMT processes were activated by MTDH to promote the metastasis of ccRCC.[6] RNA-Seq analysis in this study revealed that the NS-E peptide also significantly regulated the oncogene-related signaling pathways and inhibited the expression of chemokine genes (CXCL1, CXCL2, CXCL3, CX3CL1, etc.). This process may be mediated by NF-κB activity inhibition, but further exploration was needed. Meanwhile, other pathways related to amino acid biosynthesis and metabolism were also affected upon NS-E treatment, revealing

https://doi.org/10.1021/jacsau.3c00573
JACS Au 2024, 4, 139−149

that combining the MTDH-SND1 targeting stabilized peptides with other inhibitors may obtain more satisfying antitumor effects and provide a promising avenue to specifically treat TNBC.

To sum up, our study reported a potent peptide inhibitor (NS-E) with stronger binding affinity via structure-based optimization, providing more references for peptide design to block the MTDH-SND1 interaction. The constrained peptide delivery system further broadened the therapeutic applications of stabilized peptides and provided a feasible approach to address the gap of the poor cell permeability of biomolecules for cancer therapy.

METHODS

All cell lines used in this work were obtained from the American Type Culture Collection (ATCC) and cultured according to ATCC. The peptides were synthesized by standard solid-phase peptide synthesis and purified by high-performance liquid chromatography (HPLC). Liquid chromatography-mass spectrometry (MS) (electrospray ionization MS) was used to characterize the molecular mass of peptides. Peptides were quantified at 280 or 494 nm (FITC labeled) on NanoDrop 2000 (Thermo). Peptide affinity was evaluated by the fluorescence polarization assay using FITC-labeled peptides and recombinant protein His-SND1 (16-339) in the solution of 50 mM HEPES (pH 7.5) with 0.01% Tween 20 (v/v) and 2 mM DTT. For the pmCherry-SND1-N1 plasmid, the full-length coding sequence of SND1 was amplified from the MDA-MB-231 cDNA library and cloned into the pmCherry-N1 vector purchased in YouBio (China). Before performing the live-imaging, pmCherry-SND1-N1 plasmid was transfected into MDA-MB-231 cells and 4T1 cells, respectively. After 24 h of transfection, Wpc/NS-E (FITC labeled) was added and incubated with the cells for another 24 h.

Detailed contents of the materials and methods are shown in the Supporting Information.

ASSOCIATED CONTENT

Supporting Information

The Supporting Information is available free of charge at https://pubs.acs.org/doi/10.1021/jacsau.3c00573.

Detailed materials and methods (docking analysis, additional fluorescent statistical analysis, TEM images, cck8 assays, RNA-Seq analysis, in vivo imaging, and H&E staining analysis), primers for RT-PCR analysis, and MS and HPLC spectra (PDF)

Molecular docking information on NS-E with SND1 (PDB code: 4QMG) (PDB)

AUTHOR INFORMATION

Corresponding Authors

Yibin Kang − *Department of Molecular Biology and Ludwig Institute for Cancer Research Princeton Branch, Princeton University, Princeton, New Jersey 08544, United States*; Email: ykang@princeton.edu

Zigang Li − *State Key Laboratory of Chemical Oncogenomics, School of Chemical Biology and Biotechnology, Peking University Shenzhen Graduate School, Shenzhen 518055, China; Pingshan Translational Medicine Center, Shenzhen Bay Laboratory, Shenzhen 518118, China*; orcid.org/0000-0002-3630-8520; Email: lizg@pkusz.edu.cn

Feng Yin − *State Key Laboratory of Chemical Oncogenomics, School of Chemical Biology and Biotechnology, Peking University Shenzhen Graduate School, Shenzhen 518055, China; Pingshan Translational Medicine Center, Shenzhen Bay Laboratory, Shenzhen 518118, China*; Email: yinfeng@pkusz.edu.cn

Authors

Hailing Chen − *State Key Laboratory of Chemical Oncogenomics, School of Chemical Biology and Biotechnology, Peking University Shenzhen Graduate School, Shenzhen 518055, China*

Meimiao Zhan − *State Key Laboratory of Chemical Oncogenomics, School of Chemical Biology and Biotechnology, Peking University Shenzhen Graduate School, Shenzhen 518055, China*

Yaping Zhang − *Pingshan Translational Medicine Center, Shenzhen Bay Laboratory, Shenzhen 518118, China*; orcid.org/0000-0002-2819-6397

Jianbo Liu − *Pingshan Translational Medicine Center, Shenzhen Bay Laboratory, Shenzhen 518118, China*

Rui Wang − *Pingshan Translational Medicine Center, Shenzhen Bay Laboratory, Shenzhen 518118, China*

Yuhao An − *Pingshan Translational Medicine Center, Shenzhen Bay Laboratory, Shenzhen 518118, China*; orcid.org/0009-0006-0224-9709

Zhanxia Gao − *Pingshan Translational Medicine Center, Shenzhen Bay Laboratory, Shenzhen 518118, China*

Leying Jiang − *State Key Laboratory of Chemical Oncogenomics, School of Chemical Biology and Biotechnology, Peking University Shenzhen Graduate School, Shenzhen 518055, China*

Yun Xing − *State Key Laboratory of Chemical Oncogenomics, School of Chemical Biology and Biotechnology, Peking University Shenzhen Graduate School, Shenzhen 518055, China*

Complete contact information is available at: https://pubs.acs.org/10.1021/jacsau.3c00573

Author Contributions

Y.K., Z.L., F.Y., and H.C. conceived the project. H.C. designed and performed all the experiments. M.Z. and J.L. performed material preparation and characterization. M.Z., J.L., R.W., and Y.A. evaluated antitumor activity in vitro and analyzed the data. Y.Z., Z.G., L.J., and Y.X. evaluated antitumor activity in vivo. H.C. wrote the original draft and edited the manuscript. Y.X., Y.K., Z.L., and F.Y. reviewed and edited the manuscript. CRediT: **Hailing Chen** conceptualization, data curation, formal analysis, investigation, methodology, resources, validation, writing-original draft, writing-review & editing; **Meimiao Zhan** conceptualization, data curation, investigation, methodology, resources, validation; **Yaping Zhang** data curation, investigation, methodology, resources; **Jianbo Liu** data curation, formal analysis, methodology, resources; **Rui Wang** data curation, formal analysis, investigation, methodology, validation; **Yuhao An** data curation, formal analysis, methodology, software; **Zhanxia Gao** data curation, methodology, resources; **Leying Jiang** data curation, formal analysis, resources; **Yun Xing** data curation, formal analysis, writing-review & editing; **Yibin Kang** conceptualization, methodology, resources, writing-review & editing; **Zigang Li** conceptualization, formal analysis, funding acquisition, methodology, project administration, resources, supervision, validation, writing-review & editing; **Feng Yin** conceptualization, data curation, formal analysis, funding acquisition, investigation, methodology, project administration, resources, supervision, writing-review & editing.

https://doi.org/10.1021/jacsau.3c00573
JACS Au 2024, 4, 139−149

Notes

The authors declare the following competing financial interest(s): Y.K. is a founder and equity holder of Firebrand Thera-peutics, Inc, which is developing inhibitors against MTDH/SND1. All other authors declare they have no competing interests.

■ ACKNOWLEDGMENTS

This work was financially supported by the National Basic research program of China 973 program (2018YFA0902504 and 2021YFA0910803), the Natural Science Foundation of China grants (21977010), and the National Center for Biological Medicine Technology Innovation (NCTIB2022HS01017), the Natural Science Foundation of Guangdong Province (2022A1515010996), Shenzhen Science and Technology Program (RCJC20200714114433053, JCYJ20200109140406047, JCYJ20220818095808019, and JCYJ20210324102809026), and High-Tech Zone Development Special Project of Shenzhen (29853M-KCJ-2023-002-07). We also acknowledge financial support from the Beijing National Laboratory of Molecular Science open grant (BNLMS20160112) and the Shenzhen-Hong Kong Institute of Brain Science-Shenzhen Fundamental Research Institutions grant (2019SHIBS0004). We also thank the platform of the School of Chemical Biology and Biotechnology, Peking University Shenzhen Graduate School, Pingshan Translational Medicine Center, Shenzhen Bay Laboratory, and the Brewster Foundation to Y.K.

■ ABBREVIATIONS

ccRCC, clear cell renal cell carcinoma; CETSA, cellular thermal shift assay; CLSM, Confocal laser scanning microscopy; CPPs, cell-penetrating peptides; FITC, fluorescein isothiocyanate; HPLC, high-performance liquid chromatography; PI, propidium iodide; SPPS, solid-phase peptide synthesis; TD strategy, N-terminus aspartic acid strategy; TEM, transmission electron microscope; TNBC, triple-negative breast cancer

■ REFERENCES

(1) Nishimura, R.; Osako, T.; Okumura, Y.; Nakano, M.; Otsuka, H.; Fujisue, M.; Arima, N. Triple negative breast cancer: An analysis of the subtypes and the effects of menopausal status on invasive breast cancer. *J. Clin. Med.* **2022**, *11*, 2331−2342.

(2) Manna, D.; Sarkar, D. Multifunctional role of Astrocyte Elevated Gene-1 (AEG-1) in cancer: Focus on drug resistance. *Cancers* **2021**, *13*, 1792−1820.

(3) Shen, M.; Xie, S.; Rowicki, M.; Michel, S.; Wei, Y.; Hang, X.; Wan, L.; Lu, X.; Yuan, M.; Jin, J. F.; Jaschinski, F.; Zhou, T.; Klar, R.; Kang, Y. Therapeutic targeting of Metadherin suppresses colorectal and lung cancer progression and metastasis. *Cancer Res.* **2021**, *81*, 1014−1025.

(4) Neeli, P. K.; Sahoo, S.; Karnewar, S.; Singuru, G.; Pulipaka, S.; Annamaneni, S.; Kotamraju, S. DOT1L regulates MTDH-mediated angiogenesis in triple-negative breast cancer: intermediacy of NF-κB-HIF1α axis. *FEBS J.* **2023**, *290*, 502−520.

(5) Jariwala, N.; Rajasekaran, D.; Mendoza, R. G.; Shen, X. N.; Siddiq, A.; Akiel, M. A.; Robertson, C. L.; Subler, M. A.; Windle, J. J.; Fisher, P. B.; Sanyal, A. J.; Sarkar, D. Oncogenic role of SND1 in development and progression of hepatocellular carcinoma. *Cancer Res.* **2017**, *77*, 3306−3316.

(6) He, A.; He, S.; Huang, C.; Chen, Z.; Wu, Y.; Gong, Y.; Li, X.; Zhou, L. MTDH promotes metastasis of clear cell renal cell carcinoma by activating SND1-mediated ERK signaling and epithelial-mesenchymal transition. *Aging* **2020**, *12*, 1465−1487.

(7) Wang, Y.; Wang, X.; Cui, X.; Zhuo, Y.; Li, H.; Ha, C.; Xin, L.; Ren, Y.; Zhang, W.; Sun, X.; Ge, L.; Liu, X.; He, J.; Zhang, T.; Zhang, K.; Yao, Z.; Yang, X.; Yang, J. Oncoprotein SND1 hijacks nascent MHC-I heavy chain to ER-associated degradation, leading to impaired CD8(+) T cell response in tumor. *Sci. Adv.* **2020**, *6*, No. eaba5412.

(8) Wan, L.; Lu, X.; Yuan, S.; Wei, Y.; Guo, F.; Shen, M.; Yuan, M.; Chakrabarti, R.; Hua, Y.; Smith, H. A.; Blanco, M. A.; Chekmareva, M.; Wu, H.; Bronson, R. T.; Haffty, B. G.; Xing, Y.; Kang, Y. MTDH-SND1 interaction is crucial for expansion and activity of tumor-initiating cells in diverse oncogene- and carcinogen-induced mammary tumors. *Cancer cell* **2014**, *26*, 92−105.

(9) Shen, M.; Wei, Y.; Kim, H.; Wan, L.; Jiang, Y. Z.; Hang, X.; Raba, M.; Remiszewski, S.; Rowicki, M.; Wu, C. G.; Wu, S.; Zhang, L.; Lu, X.; Yuan, M.; Smith, H. A.; Zheng, A.; Bertino, J.; Jin, J. F.; Xing, Y.; Shao, Z. M.; Kang, Y. Small-molecule inhibitors that disrupt the MTDH-SND1 complex suppress breast cancer progression and metastasis. *Nat. Cancer* **2022**, *3*, 43−59.

(10) Shen, M.; Smith, H. A.; Wei, Y.; Jiang, Y. Z.; Zhao, S.; Wang, N.; Rowicki, M.; Tang, Y.; Hang, X.; Wu, S.; Wan, L.; Shao, Z. M.; Kang, Y. Pharmacological disruption of the MTDH-SND1 complex enhances tumor antigen presentation and synergizes with anti-PD-1 therapy in metastatic breast cancer. *Nat. Cancer* **2022**, *3*, 60−74.

(11) Blanco, M. A.; Alečković, M.; Hua, Y.; Li, T.; Wei, Y.; Xu, Z.; Cristea, I. M.; Kang, Y. Identification of staphylococcal nuclease domain-containing 1 (SND1) as a Metadherin-interacting protein with metastasis-promoting functions. *J. Biol. Chem.* **2011**, *286*, 19982−19992.

(12) Guo, F.; Wan, L.; Zheng, A.; Stanevich, V.; Wei, Y.; Satyshur, K. A.; Shen, M.; Lee, W.; Kang, Y.; Xing, Y. Structural insights into the tumor-promoting function of the MTDH-SND1 complex. *Cell Rep.* **2014**, *8*, 1704−1713.

(13) Chen, H.; Zhan, M.; Liu, J.; Liu, Z.; Shen, M.; Yang, F.; Kang, Y.; Yin, F.; Li, Z. Structure-based design, optimization, and evaluation of potent stabilized peptide inhibitors disrupting MTDH and SND1 interaction. *J. Med. Chem.* **2022**, *65*, 12188−12199.

(14) Makadia, H. K.; Siegel, S. J. Poly Lactic-co-Glycolic Acid (PLGA) as biodegradable controlled drug delivery carrier. *Polymers (Basel)* **2011**, *3*, 1377−1397.

(15) Samal, S. K.; Dash, M.; Van Vlierberghe, S.; Kaplan, D. L.; Chiellini, E.; van Blitterswijk, C.; Moroni, L.; Dubruel, P. Cationic polymers and their therapeutic potential. *Chem. Soc. Rev.* **2012**, *41*, 7147−7194.

(16) Stephen, S.; Gorain, B.; Choudhury, H.; Chatterjee, B. Exploring the role of mesoporous silica nanoparticle in the development of novel drug delivery systems. *Drug Delivery Transl. Res.* **2022**, *12*, 105−123.

(17) Liechty, W. B.; Kryscio, D. R.; Slaughter, B. V.; Peppas, N. A. Polymers for drug delivery systems. *Annu. Rev. Chem. Biomol. Eng.* **2010**, *1*, 149−173.

(18) Zhao, H.; Lin, Z. Y.; Yildirimer, L.; Dhinakar, A.; Zhao, X.; Wu, J. Polymer-based nanoparticles for protein delivery: design, strategies and applications. *J. Mater. Chem. B* **2016**, *4*, 4060−4071.

(19) Hu, F. Q.; Hong, Y.; Yuan, H. Preparation and characterization of solid lipid nanoparticles containing peptide. *Int. J. Pharm.* **2004**, *273*, 29−35.

(20) Lv, S.; Sylvestre, M.; Prossnitz, A. N.; Yang, L. F.; Pun, S. H. Design of polymeric carriers for intracellular peptide delivery in oncology applications. *Chem. Rev.* **2021**, *121*, 11653−11698.

(21) Hu, Y.; Mignani, S.; Majoral, J. P.; Shen, M.; Shi, X. Construction of iron oxide nanoparticle-based hybrid platforms for tumor imaging and therapy. *Chem. Soc. Rev.* **2018**, *47*, 1874−1900.

(22) Buse, J.; El-Aneed, A. Properties, engineering and applications of lipid-based nanoparticle drug-delivery systems: current research and advances. *Nanomedicine (Lond)* **2010**, *5*, 1237−1260.

(23) Park, S. E.; Sajid, M. I.; Parang, K.; Tiwari, R. K. Cyclic Cell-penetrating peptides as efficient intracellular drug delivery tools. *Mol. Pharmaceutics* **2019**, *16*, 3727−3743.

(24) El-Sayed, N. S.; Miyake, T.; Shirazi, A. N.; Park, S. E.; Clark, J.; Buchholz, S.; Parang, K.; Tiwari, R. Design, synthesis, and evaluation of

https://doi.org/10.1021/jacsau.3c00573
JACS Au 2024, 4, 139−149

homochiral peptides containing arginine and histidine as molecular transporters. *Molecules* **2018**, *23*, 1590−1604.
(25) Shirazi, A. N.; El-Sayed, N. S.; Mandal, D.; Tiwari, R. K.; Tavakoli, K.; Etesham, M.; Parang, K. Cysteine and arginine-rich peptides as molecular carriers. *Bioorg. Med. Chem. Lett.* **2016**, *26*, 656−661.
(26) Maiolo, J. R.; Ferrer, M.; Ottinger, E. A. Effects of cargo molecules on the cellular uptake of arginine-rich cell-penetrating peptides. *Biochim. Biophys. Acta* **2005**, *1712*, 161−172.
(27) Tünnemann, G.; Martin, R. M.; Haupt, S.; Patsch, C.; Edenhofer, F.; Cardoso, M. C. Cargo-dependent mode of uptake and bioavailability of TAT-containing proteins and peptides in living cells. *FASEB J.* **2006**, *20*, 1775−1784.
(28) Verdurmen, W. P. R.; Mazlami, M.; Plückthun, A. A quantitative comparison of cytosolic delivery via different protein uptake systems. *Sci. Rep.* **2017**, *7*, 13194.
(29) Reissmann, S. Cell penetration: scope and limitations by the application of cell-penetrating peptides. *J. Pept. Sci.* **2014**, *20*, 760−784.
(30) Shi, X.; Zhao, R.; Jiang, Y.; Zhao, H.; Tian, Y.; Jiang, Y.; Li, J.; Qin, W.; Yin, F.; Li, Z. Reversible stapling of unprotected peptides via chemoselective methionine bis-alkylation/dealkylation. *Chem. Sci.* **2018**, *9*, 3227−3232.
(31) Ma, Y.; Li, W.; Zhou, Z.; Qin, X.; Wang, D.; Gao, Y.; Yu, Z.; Yin, F.; Li, Z. Peptide-aptamer coassembly nanocarrier for cancer therapy. *Bioconjugate Chem.* **2019**, *30*, 536−540.
(32) Li, W.; Wang, D.; Shi, X.; Li, J.; Ma, Y.; Wang, Y.; Li, T.; Zhang, J.; Zhao, R.; Yu, Z.; Yin, F.; Li, Z. A siRNA-induced peptide co-assembly system as a peptide-based siRNA nanocarrier for cancer therapy. *Mater. Horiz.* **2018**, *5*, 745−752.
(33) Zhao, H.; Liu, Q. S.; Geng, H.; Tian, Y.; Cheng, M.; Jiang, Y. H.; Xie, M. S.; Niu, X. G.; Jiang, F.; Zhang, Y. O.; Lao, Y. Z.; Wu, Y. D.; Xu, N. H.; Li, Z. G. Crosslinked aspartic acids as Helix-nucleating templates. *Angew. Chem., Int. Ed. Engl.* **2016**, *55*, 12088−12093.
(34) Wan, L.; Kang, Y. Pleiotropic roles of AEG-1/MTDH/LYRIC in breast cancer *Adv. Cancer Res.* **2013**, *120*, 113−134.
(35) Emdad, L.; Das, S. K.; Dasgupta, S.; Hu, B.; Sarkar, D.; Fisher, P. B. AEG-1/MTDH/LYRIC: signaling pathways, downstream genes interacting proteins, and regulation of tumor angiogenesis. *Adv. Cancer Res.* **2013**, *120*, 75−111.
(36) Yoo, B. K.; Emdad, L.; Su, Z. Z.; Villanueva, A.; Chiang, D. Y.; Mukhopadhyay, N. D.; Mills, A. S.; Waxman, S.; Fisher, R. A.; Llovet, J. M.; Fisher, P. B.; Sarkar, D. Astrocyte elevated gene-1 regulates hepatocellular carcinoma development and progression. *J. Clin. Invest.* **2009**, *119*, 465−477.
(37) Liu, X. F.; Xiang, L.; Zhang, Y.; Becker, K. G.; Bera, T. K.; Pastan, I. CAPC negatively regulates NF-κB activation and suppresses tumor growth and metastasis. *Oncogene* **2012**, *31*, 1673−1682.
(38) Avnet, S.; Di Pompo, G.; Chano, T.; Errani, C.; Ibrahim-Hashim, A.; Gillies, R. J.; Donati, D. M.; Baldini, N. Cancer-associated mesenchymal stroma fosters the stemness of osteosarcoma cells in response to intratumoral acidosis via NF-κB activation. *Int. J. Cancer* **2017**, *140*, 1331−1345.
(39) Taniguchi, K.; Karin, M. NF-κB, inflammation, immunity and cancer: coming of age. *Nat. Rev. Immunol.* **2018**, *18*, 309−324.
(40) Bassères, D. S.; Baldwin, A. S. Nuclear factor-kappaB and inhibitor of kappaB kinase pathways in oncogenic initiation and progression. *Oncogene* **2006**, *25*, 6817−6830.
(41) Jiang, X. M.; Xu, Y. L.; Yuan, L. W.; Zhang, L. L.; Huang, M. Y.; Ye, Z. H.; Su, M. X.; Chen, X. P.; Zhu, H.; Ye, R. D.; Lu, J. J. TGFβ2-mediated epithelial-mesenchymal transition and NF-κB pathway activation contribute to osimertinib resistance. *Acta Pharmacol. Sin.* **2021**, *42*, 451−459.
(42) Massagué, J. TGFbeta in Cancer. *Cell* **2008**, *134*, 215−230.
(43) Goulet, C. R.; Pouliot, F. TGFβ Signaling in the Tumor Microenvironment. *Adv. Exp. Med. Biol.* **2021**, *1270*, 89−105.
(44) Balkwill, F. Cancer and the chemokine network. *Nat. Rev. Cancer* **2004**, *4*, 540−550.
(45) Kaur, P.; Nagaraja, G. M.; Zheng, H.; Gizachew, D.; Galukande, M.; Krishnan, S.; Asea, A. A mouse model for triple-negative breast cancer tumor-initiating cells (TNBC-TICs) exhibits similar aggressive phenotype to the human disease. *BMC Cancer* **2012**, *12*, 120.
(46) Li, P.; He, Y.; Chen, T.; Choy, K. Y.; Chow, T. S.; Wong, I. L. K.; Yang, X.; Sun, W.; Su, X.; Chan, T. H.; Chow, L. M. C. Disruption of SND1-MTDH interaction by a high affinity peptide results in SND1 degradation and cytotoxicity to breast cancer cells in vitro and in vivo. *Mol. Cancer Ther.* **2021**, *20*, 76−84.
(47) Lee, S. G.; Su, Z. Z.; Emdad, L.; Sarkar, D.; Franke, T. F.; Fisher, P. B. Astrocyte elevated gene-1 activates cell survival pathways through PI3K-Akt signaling. *Oncogene* **2008**, *27*, 1114−1121.
(48) Emdad, L.; Sarkar, D.; Su, Z. Z.; Randolph, A.; Boukerche, H.; Valerie, K.; Fisher, P. B. Activation of the nuclear factor kappaB pathway by astrocyte elevated gene-1: implications for tumor progression and metastasis. *Cancer Res.* **2006**, *66*, 1509−1516.

https://doi.org/10.1021/jacsau.3c00573
JACS Au 2024, 4, 139−149